

RSC Advances



This is an *Accepted Manuscript*, which has been through the Royal Society of Chemistry peer review process and has been accepted for publication.

Accepted Manuscripts are published online shortly after acceptance, before technical editing, formatting and proof reading. Using this free service, authors can make their results available to the community, in citable form, before we publish the edited article. This *Accepted Manuscript* will be replaced by the edited, formatted and paginated article as soon as this is available.

You can find more information about *Accepted Manuscripts* in the [Information for Authors](#).

Please note that technical editing may introduce minor changes to the text and/or graphics, which may alter content. The journal's standard [Terms & Conditions](#) and the [Ethical guidelines](#) still apply. In no event shall the Royal Society of Chemistry be held responsible for any errors or omissions in this *Accepted Manuscript* or any consequences arising from the use of any information it contains.

Exploring the mode of binding of the bioflavonoid kaempferol with B and protonated forms of DNA by spectroscopic and molecular docking study

Ankur Bikash Pradhan*, Lucy Haque, Sutanwi Bhuiya and Suman Das*

Department of Chemistry

Jadavpur University

Raja S. C. Mullick Road, Jadavpur

Kolkata 700 032

India

*Corresponding authors

Tel.: ABP: +91 9477318441

SD: +91 94 3437 3164, +91033 2457 2349; Fax: +91 33 2414 6266

E-mail:

ABP: ankurpradhan727@gmail.com

SD: sumandas10@yahoo.com

LH: lucy.haque@gmail.com

SB: s.bhuiya12@gmail.com

Abstract

Protonation-induced conformational changes in natural DNAs under the conditions of low pH at low temperature, and low ionic strength have been studied using various spectroscopic techniques. At pH 3.4, 10 mM $[\text{Na}^+]$, and at 10 °C, natural DNAs adopt an unusual and stable conformation remarkably different from the canonical B-form conformation. The protonated conformation of naturally occurring calf thymus (CT) DNA has been characterized by UV-Vis absorption and circular dichroism (CD) studies. Binding interaction of Kaempferol (KMP), a bioactive flavonoid, with B-form and protonated form of CT DNA has been explored using various spectroscopic techniques. The determined binding constant, fluorescence quenching experiment, viscosity measurement, CD study, helix melting study and molecular docking simulation confirm the groove binding of KMP with B-form and external stacking interaction with the protonated form of CT DNA. The dual fluorescence of KMP resulting from the excited state intramolecular proton transfer is modified remarkably upon binding with the protonated form of DNA. This is the first report so far where a naturally occurring flavonoid has been shown to bind to protonated form of DNA.

Keywords: Flavonoid; protonated form of DNA; DNA binding; helix melting

Introduction

The interaction of small molecules with various polymorphic forms of DNA is an active area at the interface of chemical biology and medicinal chemistry. Since the original presentation by Watson & Crick in 1953¹ of the double-helical structure of DNA, subsequent discoveries relating the structural features of this biological macromolecule not only provide insights in biology but also give the opportunity for developing effective therapeutic agents.^{2,3} The unique structural features of DNA due to the relative planar stacking of aromatic bases along the helix sugar phosphate backbone make it a particularly interesting target for drug design. Besides the canonical forms of DNA considerable effort has been expended to disclose a number of alternative DNA structures as they play important roles in different biological processes. Protonation induced structures in nucleic acid have been very significant as pH is an important factor in all biological processes. After studies on oligonucleotides using NMR it has been proposed that the first protonation sites in DNA are N3 of cytosines which lead to a unique left-handed structure with Hoogsteen base pairing (Fig. 1).⁴ The protonated-form structure is found to be distinctly different from the right-handed B-form and left-handed Z-form.^{5,6} High-resolution Raman and FTIR studies confirmed this structural model.^{7,8} Protonated DNA is unstable under physiological conditions and this limitation has led to the design of small molecules that interact with this form and stabilize it. A large number of reports are present in the literature on the biological relevance of protonated structures of natural and synthetic nucleic acids.⁸⁻¹³ Protonation of nucleic acid bases has also been shown to promote the formation of triple helices, parallel stranded structures and facilitate B–Z interconversion in synthetic alternating guanine–cytosine polynucleotides.^{6,14,15}

Given the diversity of DNA function, small molecules that selectively bind to DNA may provide novel points of therapeutic intervention. Among various DNA-binding compounds, natural products persist to be valuable and attract considerable interest since most clinical anticancer drugs are natural products or their derivatives, and most of them exert their effects by acting on DNA.^{16,17} Flavonoids, an important class of natural products, are widely distributed in fruits and vegetables. They are known to have many beneficial health effects and wide-ranging biological properties.^{18,19} Kaempferol (3,5,7-trihydroxy-2-(4'-hydroxyphenyl)-4H-1-benzopyran-4-one, hereafter KMP) (Fig. 2) is a flavonol that is present in broccoli, ginkgo biloba, fruits and vegetables.²⁰⁻²² Recently Z. Jurasekova et al. have reported a detail study about the effect of pH on some structurally related flavonoids.²³ According to them the reactivity of flavonoids depends on three main factors: (i) the C3–OH group in the C-ring; (ii) the catechol moiety in the B-ring; and (iii) the C2=C3 bond in the C-ring. Due to the lack of catechol moiety the reactivity of KMP depends on the other two factors.

Small molecules can interact differentially with different conformations of DNA. Thus a better understanding of the interaction provides an opportunity for the successful design of compounds for specific diagnostic and therapeutic purposes. It is generally accepted that there are three binding modes of small molecules to the DNA double helix: intercalation, groove binding and electrostatic binding. Electrostatic interaction is along the external DNA double helix and does not possess selectivity. Intercalation binding was first proposed by Lerman in 1961.²⁴ Groove binding is related to the two kinds of grooves in DNA, major and minor groove.

The interaction of flavonoids with nucleic acid structures plays an important role in mechanism of their actions.²⁵⁻²⁹ For these reasons, the noncovalent interactions between flavonoids and nucleic acids have attracted considerable interest and have been investigated

using several solution-phase techniques.³⁰⁻³³ Recently, Kanakis and his group found that KMP interacts with RNA and DNA.^{33,34} These discoveries motivated us to test the potential interaction of KMP with polymorphic forms of DNA. The purpose of the present work is to characterize the binding of KMP to protonated DNA to evaluate the influence of structural features on its DNA-binding properties. Interaction studies of the flavonoid with the B-form of DNA have been carried out for meaningful comparison.

Experimental Section

Materials

Both KMP and CT DNA were purchased from Sigma Aldrich Corporation (St. Louis, MO, USA). They were used without further purification. We have determined the molar extinction coefficient value of KMP by using Lambert-Beer's law. The determined molar extinction value of $14778 \text{ M}^{-1} \text{ cm}^{-1}$ at 373 nm was used to check the concentration of KMP spectrophotometrically. The solutions of KMP were kept in dark all time to avoid any light induced photochemical change. A molar extinction coefficient value of $13200 \text{ M}^{-1} \text{ cm}^{-1}$ at 260 nm in terms of base pairs was used to calculate the concentration of CT DNA solution.³⁵ No deviation from Beer's law was observed in the experimental concentration range employed in this study. Fresh solution of KMP was prepared each day for better experimental results.

Buffers

Buffers of different pH were prepared according to Gomori³⁶ and these are as follows:

1. Citrate-phosphate (CP) buffer of pH 7.0, containing a constant $[\text{Na}^+]$ of 10 mM designated as buffer-1. Nucleic acid stock solutions were prepared in this buffer.
2. Formation of the protonated form of DNA structure and its interaction with KMP were performed in CP buffer of pH 3.4, containing a constant $[\text{Na}^+]$ of 10 mM designated as buffer-2.

All buffer solutions were filtered through 0.45 μm Millipore filters to remove any particulate matter.

Methods

UV-Absorption experiments

All the UV-Vis absorbance studies were made on a Shimadzu model UV-1800 spectrophotometer (Shimadzu Corporation, Japan) in matched quartz cells of 1 cm pathlength. A thermoprogrammer was attached to it to maintain the temperature of this spectrometer by peltier effect. Spectrophotometric titrations were performed by keeping fixed concentration of KMP and varying the concentration of DNA. The changes in the absorption at the λ_{max} of flavonoid were noted at each P/D (DNA polymer/flavonoid molar ratio) till saturation was reached. To avoid any possible aggregation and prevent adsorption to the walls of the cuvette, the absorbance values have been kept at the minimum for optical studies. This spectrophotometric data then converted to titration curve of absorption versus P/D ratio. The concentrations of free and bound ligand were calculated from the derived points of the graph.

Spectrofluorimetric studies

Steady state fluorescence measurements were performed on a Shimadzu RF-5301PC spectrofluorimeter (Shimadzu Corporation, Kyoto, Japan) which was attached to a highly sensitive temperature controller. Measurements were made in fluorescence free quartz cell of path length of 1 cm. A fixed concentration of KMP was titrated by increasing concentration of DNA under constant stirring condition. All the measurements were conducted keeping an excitation and emission band pass of 5 nm.

Determination of Binding Stoichiometry

Job's continuation method³⁷ was employed to find the binding stoichiometry of KMP with CT DNA by using the fluorescence spectroscopy. At constant temperature the fluorescence intensity ($\lambda_{\text{max}}=539$ nm and 546 nm for B and protonated DNA respectively) was measured for the solution where concentration of both DNA and flavonoid were varied but the sum of their concentrations was kept constant at 10 μM . The relative difference of fluorescence intensity of KMP was plotted against the mole fraction of KMP. The break point of the plot gave the mole fraction of KMP in complex. The stoichiometry was obtained in terms of DNA:KMP $[(1-\chi_{\text{KMP}})/\chi_{\text{KMP}}]$ where χ_{KMP} denotes the mole fraction of KMP. The results reported are average of at least three experiments.

Fluorescence polarization anisotropy

The steady state fluorescence anisotropy was also measured using the same spectrofluorimeter. Steady state anisotropy (r') was defined by

$$r' = \frac{(I_{VV} - G \cdot I_{VH})}{(I_{VV} + 2G \cdot I_{VH})} \quad (1)$$

Where, G is the ratio I_{HV}/I_{HH} used for instrumental correction. I_{VV} , I_{VH} , I_{HV} and I_{HH} represent the fluorescence signal for excitation and emission with the polarizer positions set at (0,0), (0,90), (90,0) and (90,90) respectively. The excitation and emission wavelengths were fixed at 373 nm and 539 nm in buffer-1 and 367 nm and 546 nm in buffer-2 respectively. The excitation and emission slit width were fixed at 5 nm. Readings were observed 10 min after each addition to ensure the stable complex formation. Each reading was an average of five measurements. Anisotropy values were plotted as a function of increasing DNA concentration.

Fluorescence lifetime measurements

Time correlated single photon counting (TCSPC) measurements were carried out in CP buffer at 25 °C for the fluorescence decay of KMP in absence and in presence of increasing concentration

of DNA. For the TCSPC measurements, the photo-excitation was made at 370 nm using a picosecond diode laser (IBH Nanoled 07) in an IBH fluorocube apparatus. The fluorescence decay data were collected on a Hamamatsu MCP photomultiplier (R3809) and were analysed by using IBH DAS6 software using the following equation,

$$F(t) = \sum \alpha_i e^{-\left(\frac{t}{\tau}\right)} \quad (2)$$

Where, α_i is the i -th pre-exponential factor and τ is the decay time. The decay time is life time of the excited species.

Mode of binding: fluorescence quenching studies

Fluorescence quenching studies were carried out with the anionic quencher potassium iodide. Solutions of KI were mixed with the solutions of KCl in different proportions to give a fixed total ionic strength. Quenching experiments were performed at a constant P/D ratio monitoring fluorescence intensity changes at 539 nm (with B-DNA) and 546 nm (with protonated DNA) as a function of concentration of the iodide. The data were plotted in the form of Stern-Volmer equation³⁸

$$\frac{F_0}{F} = 1 + K_{SV}[Q] \quad (3)$$

Where, F_0 and F are the fluorescence intensities of the flavonoid-complex with DNA (at saturation) in the absence and in the presence of the quencher (Q) KI and K_{SV} is the Stern-Volmer quenching constant. K_{SV} is indicative of the accessibility of the bulky quencher (iodide) to the fluorophore KMP. The slope of the F_0/F versus $[KI]$ plot yields the value of K_{SV} .

Circular dichroism spectral studies

Circular dichroism (CD) measurements were carried out on a PC-driven JASCO J815 spectropolarimeter (Jasco International Co., JAPAN) attached with a temperature controller and

a thermal programmer model PFD-425L/15 interfaced in a rectangular quartz cuvette of 1 cm path length. All CD spectra were recorded in the wavelength range of 200–500 nm with a scan speed of 100 nm/min. Each spectrum was averaged from five readings. Final CD spectra were expressed in terms of molar ellipticity ($[\theta]$) in units of $\text{deg cm}^2 \text{dmol}^{-1}$ by using the software provided with the spectropolarimeter. The molar ellipticity is based on CT DNA concentration.

Viscometric study

Viscometric measurements were carried out using a Cannon-Manning semi micro dilution viscometer type 75 (Cannon Instruments Co., State College, PA, USA) submerged vertically in a constant temperature bath maintained at 25 ± 0.5 °C for B-form and at 10 ± 0.5 °C for protonated form of DNA. The molecular weight of DNA sample was estimated to be in the order of 2.25×10^5 Da with an intrinsic viscosity of 2.7 dL/g. 700 μL of 500 μM DNA solution was placed in the viscometer and aliquots of stock solution of flavonoid was directly added into the viscometer to obtain increasing D/P values. Flow times of DNA solution in the absence and in the presence of increasing concentration of dyes were measured in triplicate with an accuracy of ± 0.01 s and the relative specific viscosity was calculated using the equation:

$$\frac{\eta'_{sp}}{\eta_{sp}} = \frac{[t_{complex} - t_0]}{[t_{control} - t_0]} \quad (4)$$

Here, η'_{sp} and η_{sp} are the specific viscosity of DNA in presence and in absence of flavonoid; $t_{complex}$ and $t_{control}$ are the time of flow of complex and control solution and t_0 is the same for buffer solution as described previously.³⁵

UV optical melting study

UV optical melting measurements of protonated DNA and B-DNA in absence and in the presence of KMP were carried out on the same UV-1800 spectrophotometer by monitoring the

change in absorbance at 260 nm. The rate of heating was $0.2\text{ }^{\circ}\text{C min}^{-1}$ in the temperature range of $10\text{ }^{\circ}\text{C}$ to $70\text{ }^{\circ}\text{C}$. The melting temperature T_m , the midpoint temperature of the flavonoid bound DNA unfolding process can be estimated from the melting curves.

Molecular modeling: docking study

The native structure of DNA was taken from the RSC Protein Data Bank having PDB ID: BDL001. Docking studies were performed with the AutoDock 4.2 program, which utilizes the Lamarckian Genetic Algorithm (LGA). For the docking of the flavonoid with DNA, the required file for the flavonoid was created through the combined use of the Gaussian 09W and AutoDock 4.2 software packages. The geometry of KMP was first optimized at the DFT//B3LYP/6-31G level of theory using the Gaussian 09W suite of programs and the resultant geometry was read in the Gauss view 5 software in a compatible file format, from which the required file was generated in AutoDock 4.2. The grid box was set to 120, 120, and 120 Å along the X-, Y-, and Z-axis with a 0.403 Å grid spacing in order to recognize the binding site of KMP in CT DNA. The AutoDocking parameters used were as follows: GA population size = 150; maximum number of energy evaluations = 250000; GA crossover mode = two points. The lowest binding energy conformer was taken from 10 different conformations for each docking simulation and the resultant minimum energy conformation was applied for further analysis. The PyMOL and Mercury 3.3 software packages were used for better visualization of the docked conformations.

Results and Discussions

UV and CD spectral characteristics of B and protonated form of CT DNA

The B-form to protonated structure conformational transition was initiated by slowly adding the DNA stock solution to buffer-2, kept stirred and maintained the temperature at $10.0 \pm 0.5\text{ }^{\circ}\text{C}$. Generally the structural transition from B to protonated structure followed very fast kinetics and

was found to be completed in about 1 s. In practice, equilibrium of 5 min was allowed before measurements were performed. Characteristic UV spectra of B (curve 1) and protonated (curve 2) form are shown in Fig. 3A. At low pH there was hypochromic effect in the 260 nm absorption band. Presence of clear isosbestic point at 290 nm indicates the equilibrium of each of these duplex forms. CD spectra of B (curve 1) and protonated (curve 2) form are depicted in Fig. 3B. At pH 7.0, CT DNA exhibited conservative circular dichroic spectrum characterized by a positive CD band around 275 nm followed by a negative band at 245 nm. At pH 3.4, the conservative CD spectrum underwent remarkable changes. The 275 nm band exhibited hypochromic and bathochromic effects; concomitantly the negative band ellipticity also decreased. In case of protonated form two positive bands appear around 255 and 290 nm. Fig. 3C represents the thermal melting profiles of the two forms of CT DNA. The B-form DNA exhibited cooperative and sharp melting transitions with hyperchromicity. The melting profiles of the protonated structure in buffer-2 also showed similar cooperative and sharp transition but the thermal melting temperature (T_m) values were remarkably lower with respect to their B-form counterparts. Melting temperatures of the B-form and the protonated form of CT DNA were found to be 67 °C and 22 °C respectively. Cooperative sharp transition for the protonated form of CT DNA clearly indicates the duplex nature of DNA helix even at pH 3.4.³⁹

UV and fluorescence spectral characteristics of KMP

There are two main absorption bands in the UV spectra of KMP, which are related to the absorption of the cinnamoyl part (B+C) and the conjugated system of ring A and ring C in the molecule and can be assigned to band I (300–450 nm) and band II (250–285 nm), respectively.^{40,41} Fig. 4A shows the UV absorption spectra of KMP in CP buffer at different pH viz. 7.0 and 3.4. Recently Z. Jurasekova and his group showed that in alkaline solution the

flavonoids underwent a remarkable structural changes.²³ The chemical modification is very significant for those flavonoids which possess (i) the C3–OH group in the C-ring; (ii) the catechol moiety in the B-ring; and (iii) the C2=C3 bond in the C-ring. Here KMP does not possess any catechol moiety in the B-ring and the chemical modifications thought to be minor and dominated by deprotonation of the molecule in higher pH solution. The deprotonation of phenolic –OH in flavonoid molecule formed negative oxygenic ion, which led to a significant bathochromic shift of its UV absorption bands due to the extension of conjugation.⁴⁰⁻⁴² The maximum UV absorption wavelength (λ_{max}) of band I in CP buffer was at 367 nm in pH 3.4, and it shifted to 373 nm when the pH value of the buffer solution was changed from 3.4 to 7.0 (Fig. 4A). The fluorescence spectrum of KMP in pH 3.4 and 7.0 are presented in Fig. 4B. Photoexcitation of KMP at 373 nm shows dual emission with band maxima at 425 and 539 nm in pH 7.0, corresponding to the normal and the photoproduct tautomer, respectively.^{43,44} But no emission corresponds to the photoproduct isomer observed in pH 3.4 due to the protonation of 3-OH group in C ring and no photoproduct isomer results.

Absorbance spectral study

In order to investigate the possible binding mode and to calculate the binding constant (K_a) of KMP to B and protonated form of DNA, we have carried out the spectrophotometric titration of the complexes with naturally occurring CT DNA. The effect of increasing concentration of CT DNA on the absorption spectrum of KMP is presented in Fig. 5. The addition of both forms of CT DNA shows hypochromic effect in the UV-Vis spectra of Kaempferol. However, the extent of hypochromicity is more in presence of protonated DNA (Fig. 5B) compared to that of B-form DNA (Fig. 5A). In addition a significant bathochromic shift (~6 nm) of KMP is observed in presence of protonated DNA whereas very small change is observed in presence of B-form

DNA. The observed hypochromic and bathochromic effect in the UV-Vis spectrum of KMP is characteristic for aromatic π - π stacking interactions.⁴⁵ It is important that the changes of KMP UV-Vis spectrum induced by the addition of protonated DNA are significantly stronger than ones induced by the B-form DNA. Since KMP does not possess positive charges at pH 7, it cannot form any electrostatic interaction with negatively charged polynucleotide. In pH 3.4, due to protonation of the phenolic-OH group, KMP possess positive charge and it is believed that strong electrostatic interaction between the positively charged KMP molecules with the negatively charged polynucleotide occurs and this strong electrostatic interaction is responsible for the strong hypochromic and bathochromic effect in the UV-Vis spectrum of KMP. For protonated DNA, appearance of clear isosbestic point at 388 nm clearly indicates the equilibrium between the free and bound KMP in solution but absence of isosbestic point for the B DNA implies that 1:1 (KMP:DNA) stoichiometry is not maintained during the binding process and/or there is more than one type of binding. This prevented us to determine the binding constant from the absorption studies.

Fluorescence spectral study

KMP shows its dual fluorescence behaviour in buffer-1 while in buffer-2 the emission maxima corresponds to the photoproduct isomer is absent (Fig. 4). The emission spectrum of KMP was recorded in the wavelength range 380–700 nm with maximum around 539 nm and 546 nm when excited at 373 nm and 367 nm in buffer-1 and buffer-2 respectively (Fig. 6). Complex formation was monitored by titration studies keeping a constant concentration of the flavonoid and increasing concentration of CT DNA. With increasing concentration of B DNA a progressive enhancement in the fluorescence intensity of the normal form with a decrease in that of the tautomer species was observed and eventually reached a saturation point without any significant

shift in the wavelength maximum (Fig. 6A). But in buffer-2, upon the addition of protonated form of DNA to the aqueous solution of KMP, a new band around 546 nm corresponding to the photoproduct tautomer generates and a large enhancement in the fluorescence intensity of the tautomer species and normal form is observed (Fig. 6B). This change is associated with a red shift of ~9 nm for the tautomer emission maximum. Increase in the tautomer fluorescence species reflects that addition of protonated DNA to the KMP solution favors the excited state intramolecular proton transfer (ESIPT) process. The steady-state fluorimetric observation thus indicates a strong association between KMP and protonated form of CT DNA and reflects that KMP molecules are predominantly localized in a less polar and less protic environment within DNA. A reduction in the proticity as well as polarity favors the ESIPT process of KMP resulting in an enhancement in the tautomer formation as is evident here.⁴⁶

Based on the changes in the emission spectra of KMP upon binding to DNA, the apparent binding constant (K_a) and the binding stoichiometry (n) of DNA–KMP system can be estimated by using the following equation⁴⁷

$$\log \frac{F_o - F}{F} = \log K_a + n \log [P] \quad (5)$$

Where, F_o and F are the intensities of KMP in absence and in presence of DNA respectively and $[P]$ is the concentration of the polynucleotide. The values of K_a and n were obtained from the intercept and slope of the plot of $\log[(F_o-F)/F]$ versus $\log[P]$. The details of binding parameters obtained at 25 °C are presented in Table 1.

Stoichiometry for the association

Method of continuous variation (described earlier) was used to determine the binding stoichiometry of the complex. Resultant plot is shown in Fig. S1. Here, inflection points were observed at $\chi_{\text{KMP}} = 0.254$ and 0.31 respectively when KMP is complexed with B DNA and

protonated DNA. From these values the stoichiometry of binding were found to be ~ 3 and ~ 2 when KMP bound to B DNA and protonated DNA respectively which is in well agreement with the stoichiometry value obtained earlier by spectrofluorimetric study.

Mode of binding: fluorescence quenching experiments

Fluorescence quenching experiment is a very well-known method to investigate the mode of binding of small molecules to nucleic acid structures.³⁵ In the complex, molecules that are inserted between bases/base pairs may not be accessible to the quencher while the molecules that are free or bound on the surface of the DNA may be readily available to an anionic quencher. The negative charges on the phosphate groups at the helix surface restrict the insertion of an anionic quencher into the interior of the helix. Hence, a little or no quenching may be observed in presence of an anionic quencher if the binding involves intercalation/strong stacking. As a result, the magnitude of the Stern–Volmer quenching constant (K_{sv}) of the ligands that are bound inside will be lower than that of the free molecules. It has been observed that binding to protonated DNA resulted in an increase of the fluorescence intensity of KMP while fluorescence intensity of KMP decreases in presence of B DNA (Fig. 6). Fig.S2 represents the Stern-Volmer plots of KMP in the absence and presence of B DNA and protonated DNA. Representative K_{sv} values for free and bound KMP are presented in Table 2. These results indicate that the KMP is very much less accessible to the quencher when it binds to protonated DNA or in other words it is considerably protected and sequestered away from the solvent suggesting intercalative binding or strong stacking interaction with protonated DNA. While in case of B DNA, the effect is small indicating that the mode may not be intercalative or there may be groove binding between KMP and B form of DNA.

Viscometric study

Higher viscosity of a solution means that there are attractive forces within the solution (thereby counteracting the movement of different "layers" within the liquid). According to the classical concept of intercalation, when a drug intercalates between the base pairs of DNA, its presence forces the base pairs away from each other. This causes unwinding of the double helix causing a given amount of DNA to lengthen. This in turn increases the viscosity of the solution. So for an intercalating agent, the attraction between DNA and intercalator is greater than that of free DNA in solution. This could be due to the opening of double-stranded, which definitely will alter the mutual interactions of the molecules, and this goes obviously in the direction of more intense interactions. Groove-binding agent, at least the ones do not cause any disruption of the double helical structure hence do not affect the viscosity. The change in viscosity with the addition of flavonoid into DNA solution is presented in Fig. 7. Our results indicate that in both cases (B and protonated form of DNA) with the addition of KMP there are negligible changes in the viscosity. However the result with the B form is quite expected as viscosity does not alter in case of groove binding. But in case of protonated form almost negligible change in viscosity ruled out the probability of intercalation as in case of intercalation viscosity of the DNA solution increases significantly. So there must be strong stacking interaction between the protonated DNA and KMP which reflects their high binding constant.

CD studies on the binding of KMP to the B-form and protonated form of DNA

CD spectral changes of B-form and protonated form of CT DNA with KMP are presented in Fig. 8. The characteristic B-form spectrum of CT DNA undergoes a small change in presence of KMP, manifested by small increase in the ellipticity of the positive band with increasing concentration of the flavonoid (Fig. 8A). There was absence of appreciable shift of the bands in presence of flavonoid. The CD spectrum of protonated form of CT DNA was strongly perturbed

on interaction with KMP. The changes are depicted in Fig. 8B. According to Fig. 8B, the broad positive band around 290 nm was decreased in ellipticity and became a sharp band without any significant shift in wavelength. Concomitantly, ellipticity of another positive band around 260 nm was also decreased upto saturation and the negative band at 245 nm was blue shifted and enhanced in ellipticity. A plausible explanation of these changes is the disruption of stacking contacts of the bases. These changes may thus reflect local unwinding of the DNA helical backbone and changes in relative orientation of the bases to accommodate the flavonoid molecules. It can be observed that the perturbation of CD spectrum is more pronounced in presence of protonated DNA compared to that of B DNA. This implies that binding of KMP causes the greater perturbation to the protonated DNA strands. KMP is a planar and achiral molecule in nature and as a result it is CD inactive. Appearance of extrinsic CD band in a wavelength region where the DNA has no absorption band clearly indicates the asymmetric arrangement of the flavonoid that has been intercalated into the DNA base pairs or stacked on the DNA strands. However the extent of induced spectra of KMP which arises due to the B DNA is negligibly small compared to the protonated DNA. This clearly indicates that KMP strongly binds to protonated DNA and the binding is probably intercalative/stacking interaction in nature whereas in case of B DNA the binding is groove binding.

Fluorescence polarization anisotropy measurements

Fluorescence anisotropy values provide important information about the nature of the environment of fluorophores. Factors which cause any change in shape, size and rigidity of a probe alters the observed anisotropy. Since increase in the rigidity of the environment of fluorophore causes an increase in the fluorescence anisotropy we have monitored anisotropy of KMP in presence of increasing concentration of both forms of DNA. Fig. S3 shows the variation

of fluorescence anisotropy of KMP with increasing concentration of B and protonated form of DNA. It has been found that the fluorescence polarization upon binding of KMP to the B DNA shows a value of 0.182 at saturation against a value of 0.078 for free KMP under identical condition; while for protonated DNA the value is 0.352 at saturation against a value of 0.081 for the free flavonoid. Thus in presence of B DNA, anisotropy value became ~ 2.3 -fold while it becomes ~ 4.3 -fold in presence of protonated DNA. This clearly indicates that the flavonoid is trapped in a motionally restricted region within both forms of DNA. Comparatively less extent of change in case of B DNA clearly indicates a less restriction of motion of the dye in the B DNA environment.

Fluorescence lifetime measurements

The fluorescence decay profiles of KMP in absence and in presence of B-form and protonated form of DNA are shown in Fig. 9. The lifetimes and their weight obtained from the best fittings to the decay profile are presented in Table 3. When a monoexponential fit did not adjust well, biexponential fittings were used. The results show that KMP have biexponential decays in pH 7.0 correspond to the normal and photoproducted isomer but in pH 3.4 the decay was monoexponential due to the absence of photoproducted isomer. In presence of either form of DNA the decays are biexponential in nature. In case of free KMP in pH 7.0 and 3.4 the life time was 0.79 and 0.91 ns respectively. The life time of the first component remains almost unchanged in presence of either form of the DNA while for the second component the change was 3.16 ns to 5.26 ns for B-form DNA and 3.56 to 8.56 ns for protonated DNA at saturation. Our data clearly indicate that there is partitioning of the dyes in two environments; one is free and the other is in bound form. Increase in values of lifetime showed strong binding of the compound to the polymer and the binding is stronger in case of protonated DNA.

Thermal melting study of KMP–DNA complexation

Stabilization of B-form and protonated form structures was monitored in the presence of KMP using helix melting study. Stabilization of the helix because of the intercalation or stacking of probes results in an increase in the helix melting temperature of the DNA whereas for groove binding relatively small increase in melting temperature occurs.⁴⁸⁻⁵⁰ Melting temperature (T_m) is the temperature at which 50% of double stranded DNA becomes single stranded and it is obtained from the midpoint of the absorbance *versus* temperature melting profile. We have examined the T_m of both the B DNA and protonated DNA in native form as well as in presence of KMP (Fig. 10). In presence of KMP at a fixed D/P of 0.6, stabilization of B-form of CT DNA was observed with very small change ($\sim 5^\circ\text{C}$) in the T_m of the transition. But at the said D/P ratio the extent of stabilization of the protonated form of DNA was $\sim 20^\circ\text{C}$ (T_m changes from 22.9°C to 42.9°C upon binding to KMP). Fig. 10C shows the variation of T_m as a function of D/P molar ratio. The relation between T_m and dye/duplex ratio is essentially linear, with a slope of $3.8^\circ\text{C}/(\text{D/P})$ for protonated DNA-KMP complex, which is nearly six times higher than that for the B DNA-KMP complex, $0.66^\circ\text{C}/(\text{D/P})$. The effect of KMP on T_m is the result of three physical effects.⁵¹ First, the positively charged flavonoid molecules (when the 3-OH group in C ring is protonated in pH 3.4 buffer) screen the negatively charged phosphates in the DNA backbone. Second, the presence of the flavonoid's aromatic rings enhances stacking interactions. Third, by locally stretching/unwinding the double helix flavonoid molecules reduce the charge density per unit length along the backbone. So these melting data clearly indicate a strong binding of KMP in between the base pairs of protonated DNA structures. On the other hand, with the B DNA less stabilization of the duplex in presence of KMP was observed. Inappreciable change in T_m of the B DNA upon binding with KMP establishes the groove binding between the two. An increase in

T_m of the DNA (as a result of intercalation or stacking) or inappreciable change in T_m (as a result of groove binding) is consistent with the literature.^{35,46,52-54}

Modeling of KMP binding site in DNA: blind docking study

In order to understand the efficacy of a biologically active molecule to function as therapeutic agent, the knowledge of its binding location in the nucleic acid is very crucial and important. Herein, the flavonoid binding site in DNA has been explored on the basis of blind docking simulation performed according to the protocol described in the method section. The strategy of AutoDock-based blind docking includes a search over the entire surface of the DNA for binding sites thereby indulging in an unbiased result, and hence has rightfully been described as “very encouraging” in a recent review and has also been receiving enormous attention from various research groups.⁵⁵⁻⁵⁷ The docked pose displayed in Fig. 11 reveals the minor groove of the B DNA and the sugar phosphate strands (stacking interaction) of the protonated DNA to be the favorable binding site for the flavonoid KMP. The right panels of Fig. 11 mark the DNA bases in near vicinity (within 4 Å) of the flavonoid. The KMP–B DNA complex could fit well into the minor groove of the DNA with a binding site of four base pairs, preferentially involving the A-C residues (Fig. 11C). In case of KMP-protonated DNA, the complex could fit into the region where extensive electrostatic as well as hydrogen bonding occurs with the sugar phosphate strands and the G-C⁺ base pair as revealed by the docked structure (Fig. 11F). The lengths of hydrogen bond with adenine and cytosine bases (Fig. 11C) are 3.5, 2.4 and 2.8 Å respectively for B-DNA. For protonated-DNA, the lengths of hydrogen bond with guanine and protonated cytosine bases are 3.7 and 2.4 Å respectively. Thus the significant change in the spectra of KMP in presence of protonated DNA likely caused by extensive stacking interactions. Upon binding, KMP is thought to bind to the Hoogsteen face of G37 and C⁺39 (Fig. 11F). The KMP molecule

also interacts with the phosphate groups of T22 and C⁺23 via hydrogen bonding and electrostatic interaction and these ionic interactions have been shown to be important in achieving high affinity. Generally positively charged moieties enhance affinity by interacting with the phosphate backbone.⁵⁴ Since in pH 3.4 KMP bears a positive charge on ring C, the result is consistent with the reported data. This array of hydrogen-bonding and stacking interactions may prove suitable for tight, selective recognition by small molecule binders.

Conclusion

The present work provides an explicit picture on the interaction of the antioxidant flavonoid KMP with B form and protonated form of CT DNA. The dual fluorimetric behaviour of the flavonoid modified remarkably upon binding to the protonated form of DNA as compared to the B DNA. A series of studies involving absorption, steady-state fluorescence, fluorescence anisotropy, fluorescence quenching, viscosity, CD, helix melting study and molecular docking simulation study unambiguously establish that KMP binds to B DNA in a minor groove binding fashion in contrast to the external stacking interaction when KMP binds to protonated form of DNA.

Acknowledgement

The authors sincerely acknowledge Professor Nitin Chattopadhyay for providing his laboratory facilities whenever required. ABP, LH and SB thank the University Grants Commission, Government of India, for the award of Junior Research Fellowship.

References

1. J. D. Watson and F. H. C. Crick, *Nature*, 1953, **171**, 737-738.
2. P. B. Dervan, *Biorg. Med. Chem.*, 2001, **9**, 2215–2235.
3. M. Maiti and G. S. Kumar, *Med. Res. Rev.*, 2007, **27**, 649–695.

4. K. Hoogsteen, *Acta Crystallogr. Sec. A*, 1963, **16**, 907.
5. R. J. Topping, M. P. Stone, C. K. Brush and T. M. Harris, *Biochemistry*, 1988, **27**, 7216-7222.
6. H. Robinson, G. A. van der Marel, J. H. van Boom and A. H. J. Wang, *Biochemistry*, 1992, **31**, 10510-10517.
7. H. A. Tajmir-Riahi, J. F. Neault and M. Naoui, *FEBS Lett.*, 1995, **370**, 105-108.
8. G. M. J. Segers-Nolten, N. M. Sijtsema and C. Otto, *Biochemistry*, 1997, **36**, 13241-13247.
9. G. S. Kumar, S. Das, K. Bhadra and M. Maiti, *Bioorg. Med. Chem.*, 2003, **11**, 4861-4870.
10. K. Bhadra, G. S. Kumar, S. Das, M. Islam and M. Maiti, *Bioorg. Med. Chem.*, 2005, **13**, 4851-4863.
11. N. A. Siegfried, B. O'Hare and P. C. Bevilacqua, *Biochemistry*, 2010, **49**, 3225-3236.
12. I. T. Suydam, S. D. Levandoski and S. A. Strobel, *Biochemistry*, 2010, **49**, 3723-3732.
13. A. G. Kudrev, *Biofizika*, 2012, **57**, 422-431.
14. R. J. Topping, M. P. Stone, C. K. Brush and T. M. Harris, *Biochemistry*, 1988, **27**, 7216-7222.
15. S. Das, S. Kundu and G. S. Kumar, *DNA & Cell Biol.*, 2011, **30**, 525-535.
16. D. J. Newman, G. M. Cragg and K. M. Snader, *J. Nat. Prod.*, 2003, **66**, 1022-1037.
17. W. C. Tse and D. L. Boger, *Chem. Biol.*, 2004, **11**, 1607-1617.
18. B. H. Havsteen, *Pharmacol. Ther.*, 2002, **96**, 67-202.
19. W. Ren, Z. Qiao, H. Wang, L. Zhu and L. Zhang, *Med. Res. Rev.*, 2003, **23**, 519-534.
20. S. Karakaya and E. L. Sedef Nehir, *Food Chem.*, 1999, **66**, 289-292.

21. I. Crespo, M. V. García-Mediavilla, B. Gutiérrez, S. Sánchez-Campos, M. J. Tuñón and J. González-Gallego, *British J. Nutr.*, 2008, **100**, 968-976.
22. D. Bücherl, *Isolation of kaempferol glycosides from Ginkgo biloba leaves and synthesis, identification and quantification of their major in vivo metabolites*; University of Regensburg: Dissertation, 2014.
23. Z. Jurasekova, C. Domingo, J. V. Garcia-Ramosb and S. Sanchez Cortes, *Phys. Chem. Chem. Phys.*, 2014, **16**, 12802-12811.
24. L. S. Lerman, *J. Mol. Biol.*, 1961, **3**, 18-30.
25. B. B. Das, N. Sen, A. Roy, S. B. Dasgupta, A. Ganguly, B. C. Mohanta, B. Dinda and H. K. Majumder, *Nucl. Acids Res.*, 2006, **34**, 1121-1132.
26. O. J. Bandele and N. Osheroff, *Biochemistry*, 2007, **46**, 6097-6108.
27. T. J. Zwang, K. Singh, M. S. Johal and C. R. Selassie, *J. Med. Chem.*, 2013, **56**, 1491-1498.
28. Y. M. Temerk, M. S. Ibrahim, M. Kotb and W. Schuhmann, *Anal. Bioanal. Chem.*, 2013, **405**, 3839-3846.
29. Z. Zhu, C. Li and N. Li, *Microchem. J.*, 2002, **71**, 57-63.
30. S. Y. Bi, C. Y. Qiao, D. Q. Song, Y. Tian, D. J. Gao, Y. Sun and H. Q. Zhang, *Sens. Actua. B*, 2006, **119**, 199-208.
31. W. Bocian, R. Kawecki, E. Bednarek, J. Sitkowski, A. Ulkowska and L. Kozerski, *New J. Chem.*, 2006, **30**, 467-472.
32. C. D. Kanakis, P. A. Tarantilis, M. G. Polissiou, S. Diamantoglou and H. A. Tajmir-Riahi, *Cell Biochem. Biophys.*, 2007, **49**, 29-36.

33. C. D. Kanakis, P. A. Tarantilis, M. G. Polissiou, S. Diamantoglou and H. A. Tajmir-Riahi, *J. Biomol. Struct. Dyn.*, 2005, **22**, 719-724.
34. C. D. Kanakis, P. A. Tarantilis, M. G. Polissiou and H. A. Tajmir-Riahi, *DNA & Cell Biol.*, 2006, **25**, 116-123.
35. S. Das and G. S. Kumar, *J. Mol. Struct.*, 2008, **872**, 56-63.
36. G. Gomori, *Methods in Enzymol.*, 1955, **1**, 138-146.
37. P. Job, *Annali di Chim. Appl.*, 1928, **9**, 113-203.
38. J. R. Lakowicz, *Principles of Fluorescence Spectroscopy*; Plenum Press: New York, U.S.A., 2006.
39. K. Bhadra, G. S. Kumar, S. Das, M. Islam and M. Maiti, *Bioorg. Med. Chem.*, 2005, **13**, 4851-4863.
40. F. Zsila, Z. Bikadi and M. Simonyi, *Biochem. Pharmacol.*, 2003, **65**, 447-456.
41. L. Huang and D. Q. Yu, *The Application of Ultra-Violet Spectroscopy in Organic Chemistry*; Scientific Press: Beijing, 1988.
42. S. Tommasini, M. L. Calabro and P. Donato, *J. Pharma. Biomed. Anal.*, 2004, **35**, 389-397.
43. M. Kasha, *J. Chem. Soc., Faraday Trans.*, 1986, **82**, 2379-2392.
44. S. Chaudhuri, K. Basu, B. Sengupta, A. Banerjee and P. K. Sengupta, *Luminescence*, 2008, **23**, 397-403.
45. G. Dougherty and J. R. Pilbrow, *Int. J. Biochem.*, 1984, **16**, 1179-1192
46. B. Jana, S. Senapati, D. Ghosh, D. Bose and N. Chattopadhyay, *J. Phys. Chem. B*, 2012, 116, 639-645.
47. J. F. Li and C. Dong, *Spectrochim. Acta Part A*, 2009, **71**, 1938-1943.

48. B. K. Paul and N. Guchhait, *J. Phys. Chem. B*, 2011, **115**, 11938-11949.
49. N. Shahabadia, N. Fatahib, M. Mahdavia, Z. K. Nejada and M. Pourfoulada, *Spectrochim. Acta Part A*, 2011, **83**, 420-424.
50. C. V. Kumar, R. S. Turner and E. H. Asuncion, *J. Photochem. Photobiol. A*, 1993, **74**, 231-238.
51. V. A. Bloomfield, D. M. Crothers and J. Ignacio Tinoco, *Nucleic Acids Structures, Properties and Functions*; University Science Books: Sausalito, CA, 2000.
52. A. Larsson, C. Carlsson, M. Jonsson and N. Albinsson, *J. Am. Chem. Soc.*, 1994, **116**, 8459-8465.
53. M. H. David-Cordonnier, W. Laine, A. Lansiaux, F. Rosu, P. Colson, E. de Pauw, S. Michel, F. Tillequin, M. Koch, J. A. Hickman, A. Pierré and C. Bailly, *Mol. cancer Ther.*, 2005, **4**, 71-80.
54. J. R. Thomas and P. J. Hergenrother, *Chem Rev.*, 2008, **108**, 1171-1224.
55. S. J. Campbell, N. D. Gold, R. M. Jackson and D. R. Westhead, *Curr. Opin. Struct. Biol.*, 2003, **13**, 389-395.
56. S. Monti, I. Manet, F. Manoli and G. Marconi, *Phys. Chem. Chem. Phys.*, 2008, **10**, 6597-6606.
57. A. Ganguly, B. K. Paul, S. Ghosh, S. Dalapati and N. Guchhait, *Phys. Chem. Chem. phys.*, 2014, **16**, 8465-8475.

Figure Legends

Fig. 1. Structure of Watson–Crick pairing and Hoogsteen pairing scheme in the DNA base pair.

Fig. 2. Chemical structure of Kaempferol (KMP).

Fig. 3. Representative (A) UV spectra, (B) CD spectra and (C) thermal melting profiles of B form (Curve 1, at pH 7.0) and protonated form (Curve 2, at pH 3.4) of CT DNA (10 μM) in CP buffer of 10 mM $[\text{Na}^+]$ at 25 $^\circ\text{C}$ and 10 $^\circ\text{C}$ respectively.

Fig. 4. Representative (A) UV spectra and (B) Fluorescence emission spectra of KMP in 10 mM CP buffer of pH 7.0 (curve 1) and pH 3.4 (curve 2) at 25 $^\circ\text{C}$ and 10 $^\circ\text{C}$ respectively.

Fig. 5. Absorption spectra of KMP in presence CT DNA: (A) Spectra 1–6 denote the absorption spectrum of KMP (8.15 μM) treated with 0, 19.37, 49.97, 76.36, 124.41 and 178.37 μM of CT DNA in buffer-1 at 25 $^\circ\text{C}$ and (B) spectra of 1–5 denote the absorption spectrum of KMP (8.0 μM) treated with 0, 16.00, 32.00, 64.00 and 80.00 μM of CT DNA in 10 mM CP buffer-2 at 10 $^\circ\text{C}$.

Fig. 6. Fluorescence spectra of KMP in presence of CT DNA: (A) Spectra 1-6 denote the fluorescence spectrum of KMP (4.93 μM) treated with 0, 3.89, 12.06, 27.23, 38.15 and 50.12 μM of CT DNA in buffer-1 at 25 $^\circ\text{C}$ and (B) spectra 1–9 denotes the fluorescence of KMP (4.93 μM) treated with 0, 2.56, 6.42, 12.25, 25.56, 37.27, 52.52, 67.74 and 85.16 μM of CT DNA in buffer-2 at 10 $^\circ\text{C}$. Inset of both figure represent their respective binding plot.

Fig. 7. A plot of change of relative specific viscosity of B-form (●) and protonated form (●) of CT DNA with increasing concentration of KMP in buffer-1 at 25 $^\circ\text{C}$ and buffer-2 at 10 $^\circ\text{C}$ respectively. The concentration of CT DNA was 500 μM .

Fig. 8. CD spectra of CT DNA (100.0 μM , curve1) treated with (A) 12.37, 30.87 and 67.12 μM of KMP (curves 2–4) in buffer-1 at 25 $^{\circ}\text{C}$; (B) CT DNA (100.0 μM , curve (1) treated with 6.187, 12.37, 24.71, 43.18, 55.46 and 67.72 μM of KMP (curves 2–6) in buffer-2 at 10 $^{\circ}\text{C}$.

Fig. 9. Time-resolved fluorescence decay curves (logarithm of normalised intensity versus time in ns) for KMP in absence and in presence of increasing concentration of (A) B DNA at 25 $^{\circ}\text{C}$ in buffer-1 and (B) protonated DNA at 10 $^{\circ}\text{C}$ in buffer-2. A: Profiles for free 12.65 μM KMP (●) treated with 13.98 μM (●), 69.69 μM (●) and 161.81 μM (●) of B DNA. B: Profiles for free 12.65 μM KMP (●) treated with 12.65 μM (●), 50.6 μM (●) and 126.5 μM (●) of protonated DNA.

Fig. 10. Representative thermal melting profiles (absorbance change at 260 nm versus temperature) of B-form (A) and protonated form (B) of CT DNA in buffer-1 and buffer-2 respectively in presence of KMP. (A) Thermal melting profiles of B form CT DNA (●) and in presence of KMP at D/P values 0.2(●), 0.4(●) and 0.6(●) respectively (B) Thermal melting profiles of protonated form CT DNA (●) and in presence of KMP at D/P values 0.2(●), 0.4(●) and 0.6(●) respectively. (C) Melting temperature, T_m , as a function of the D/P molar ratio for B DNA(●) and protonated DNA(●) in presence of KMP.

Fig. 11. Stereo view of the docked conformation of the flavonoid KMP with (A) B form and (D) protonated form of CT DNA. The site of the interaction of the flavonoid is magnified on the right panel in the near vicinity (within 4.0 \AA) of the flavonoid at the interaction site.

TABLE 1

Binding parameters for the interaction of KMP with B and protonated DNA in buffer-1 and buffer-2 respectively obtained from spectrofluorimetry.^a

Parameters	System	Methods	Values
$K_a \times 10^{-4} (M^{-1})$	KMP- B DNA	Spectrofluorimetry	1.52±0.10
	KMP- H DNA	Spectrofluorimetry	5.68±0.07
n (stoichiometry)	KMP- B DNA	[A] Spectrofluorimetry	2.95±0.05
	KMP- H DNA		2.12±0.01
	KMP- B DNA	[B] Job's method	3.08±0.04
	KMP- H DNA		1.78±0.01

^a Average of three determinations

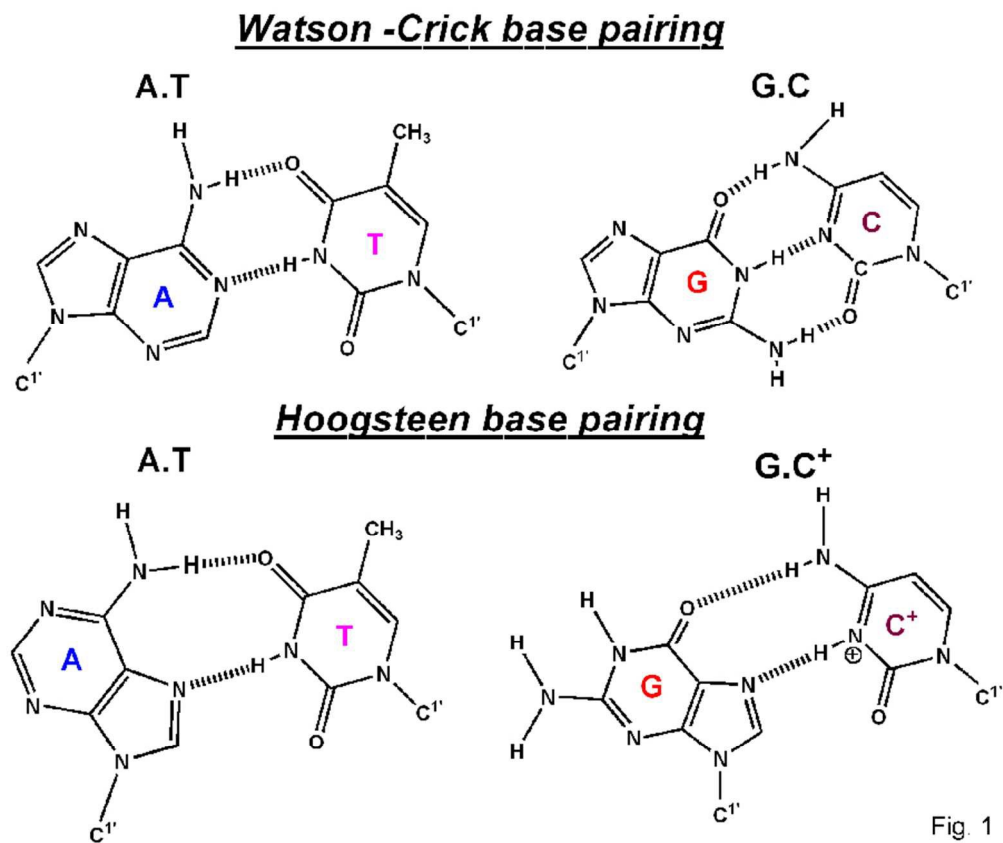
TABLE 2Comparison of K_{SV} Values for KMP in different CT DNA environments

Fluorophore	Polymer	K_{sv} (free) (L mol⁻¹)	K_{sv} in CT DNA environment (L mol⁻¹)	Relative reduction in K_{sv} (%)
KMP	B DNA	18.32	12.33	32.69
	Protonated DNA	22.01	5.68	74.19

TABLE 3

Life time data for KMP in absence and in presence of B and protonated forms of CT DNA in buffer-1 and buffer-2 respectively.

Dye	[DNA]/ [Flavonoid]	τ_1 (ns)	τ_2 (ns)	CHISQ	
KMP	B-form	0.0	0.79	3.16	1.11
		1.11	0.82	3.98	0.91
		2.58	0.87	4.81	1.10
		5.51	0.88	5.01	1.21
		8.43	0.88	5.05	0.99
		12.79	0.89	5.16	1.10
		18.56	0.89	5.26	1.19
	Protonated form	0.0	0.91	3.56	0.99
		1.0	1.03	3.68	1.11
		2.0	1.11	5.51	0.99
		4.0	1.16	6.82	1.12
		6.0	1.21	8.11	1.10
		8.0	1.23	8.49	0.91
		10.0	1.24	8.56	1.12



76x64mm (300 x 300 DPI)

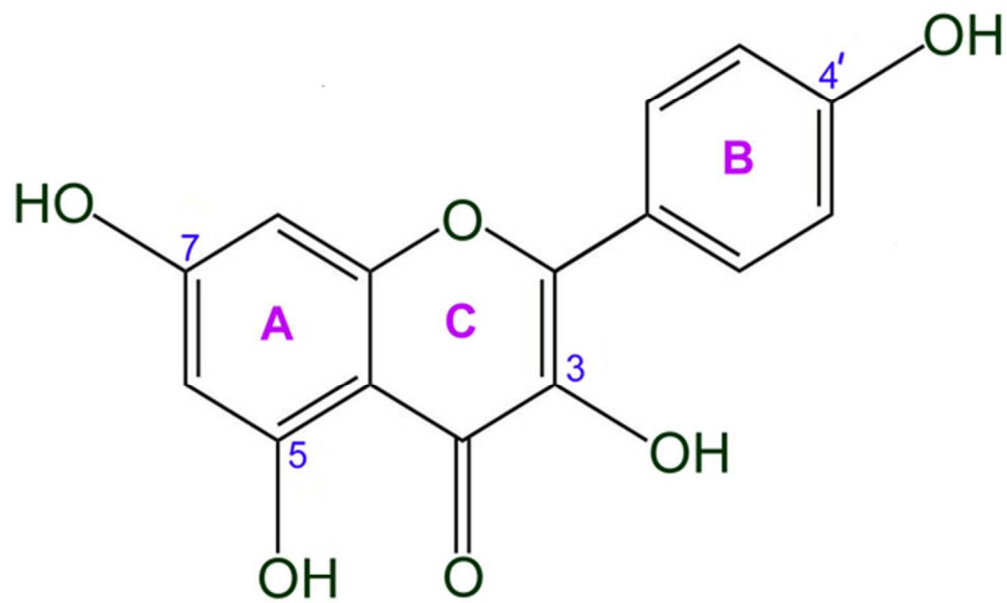


Fig. 2

50x33mm (300 x 300 DPI)

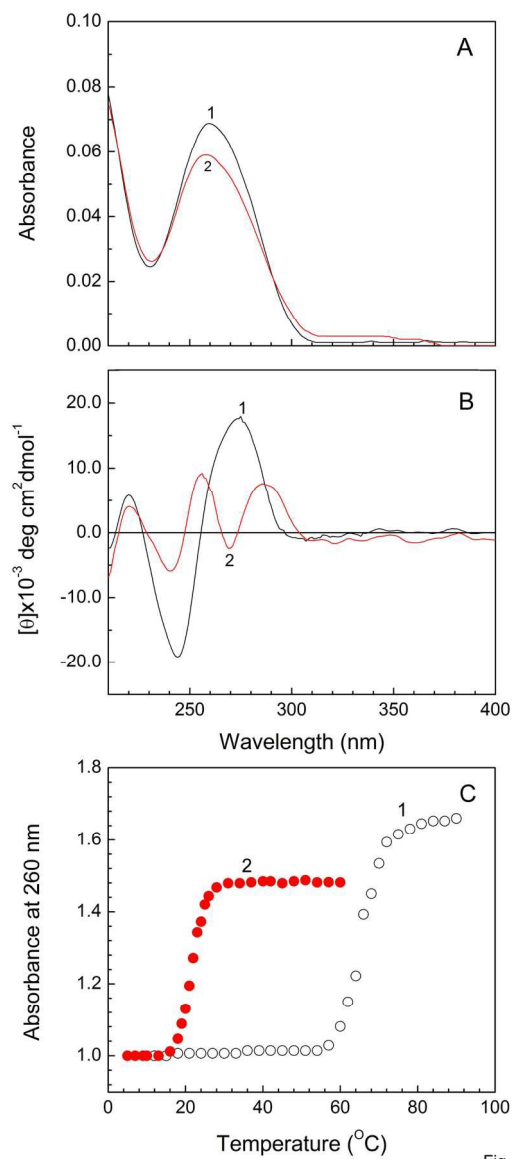


Fig. 3

152x330mm (300 x 300 DPI)

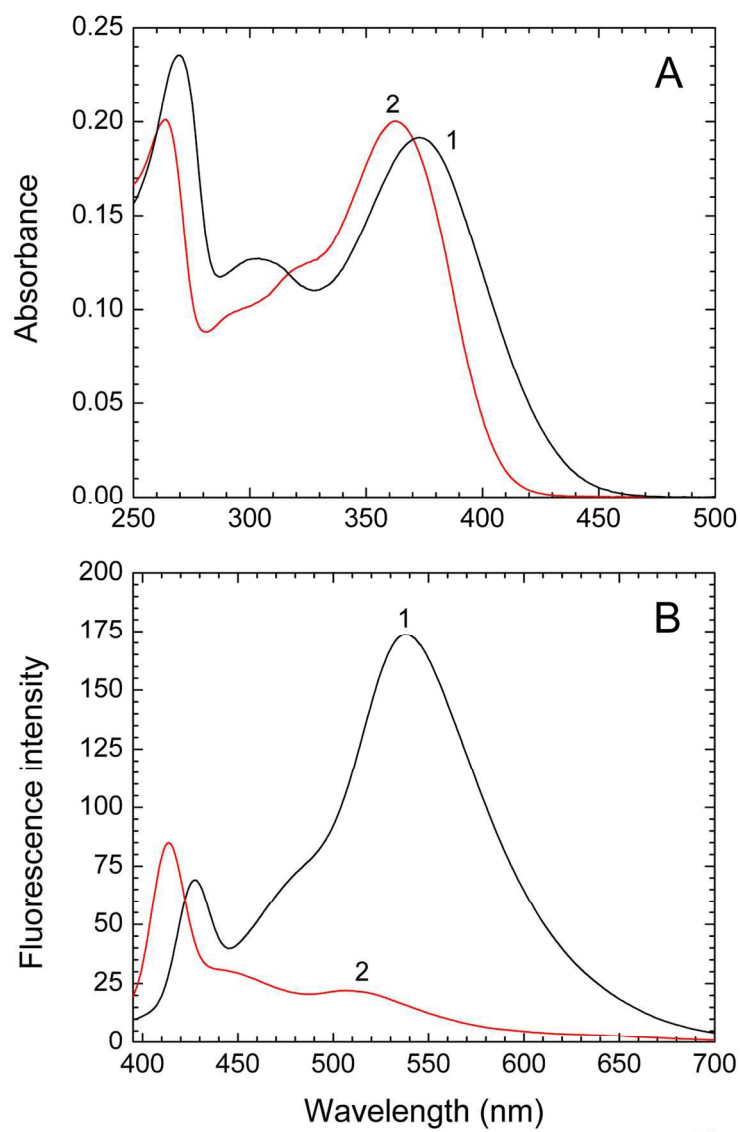


Fig. 4

127x191mm (300 x 300 DPI)

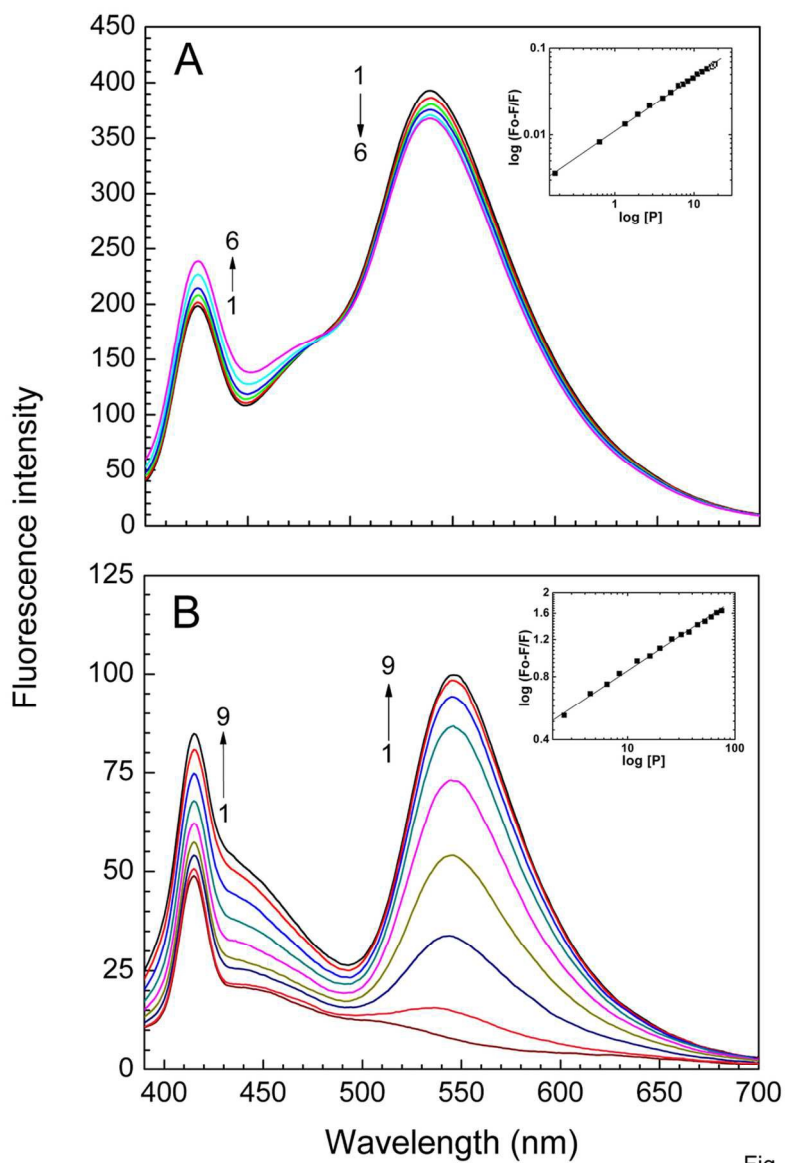


Fig. 6

101x145mm (300 x 300 DPI)

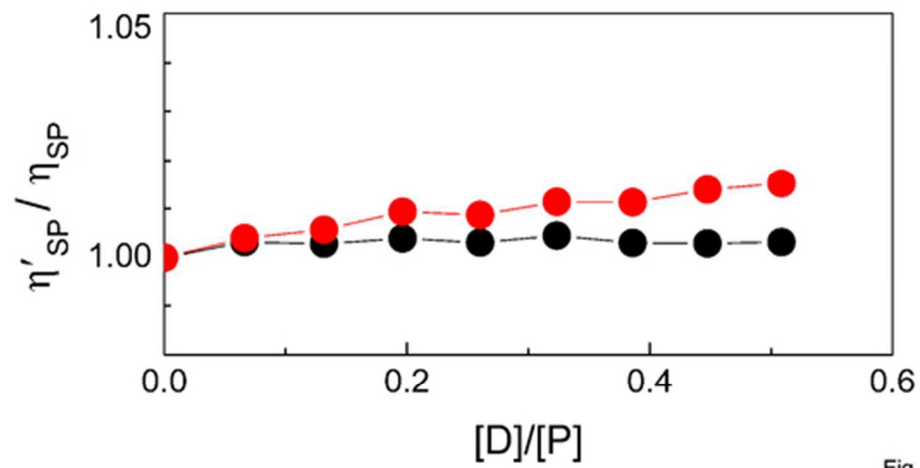


Fig. 7

49x25mm (300 x 300 DPI)

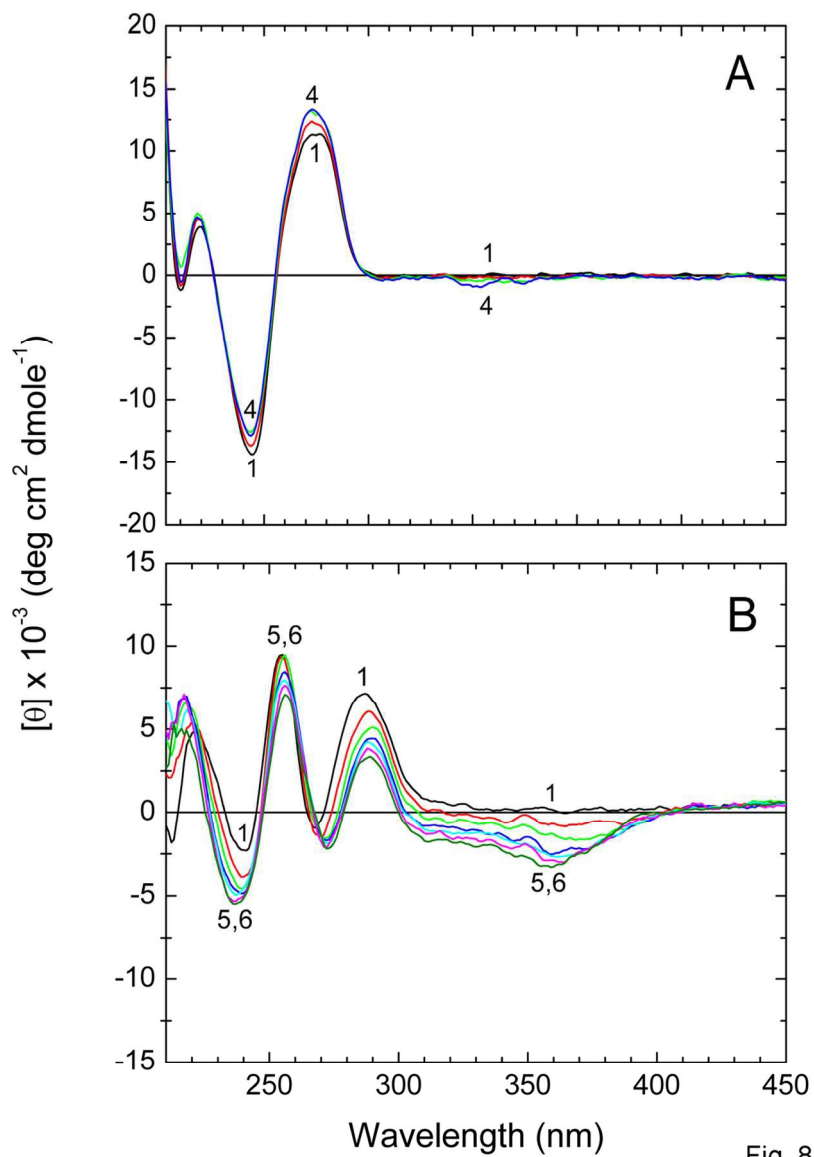
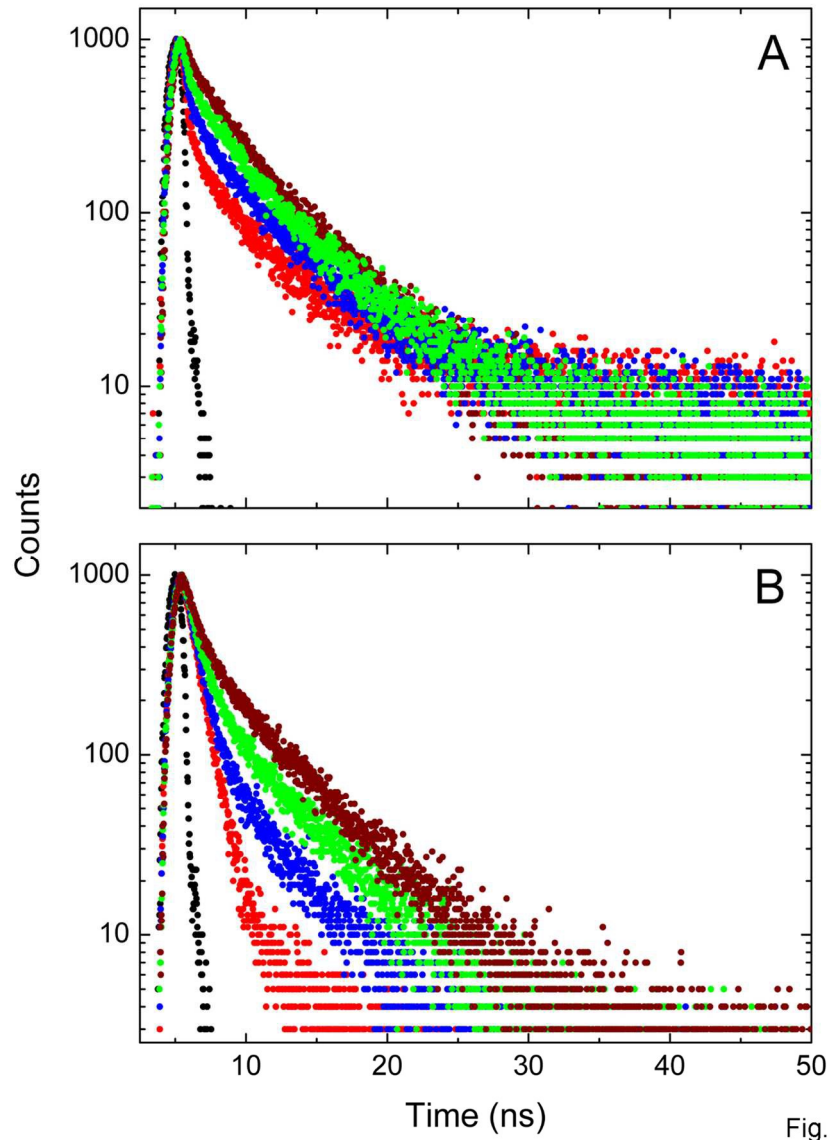
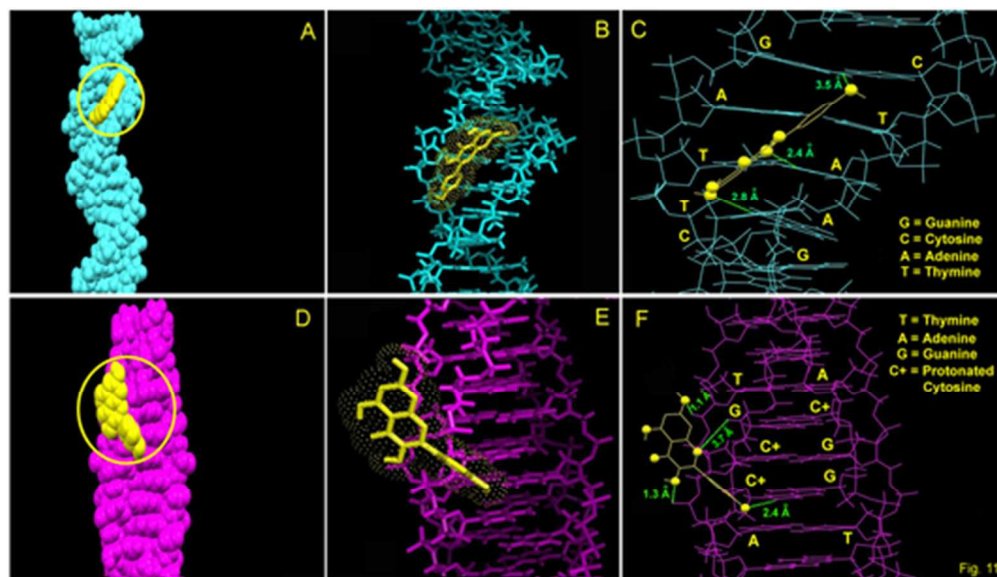


Fig. 8

110x157mm (300 x 300 DPI)



113x156mm (300 x 300 DPI)



45x25mm (300 x 300 DPI)

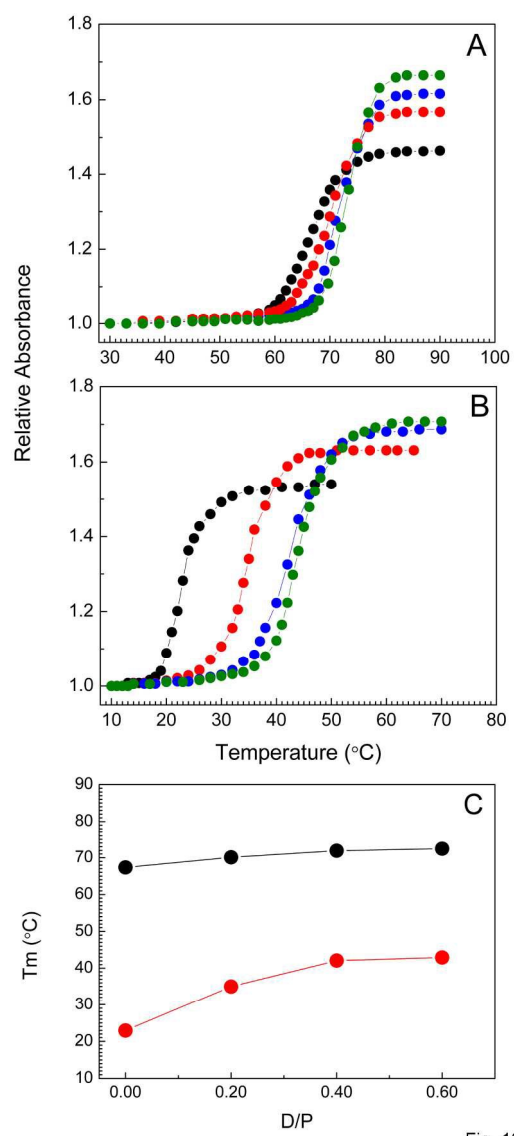
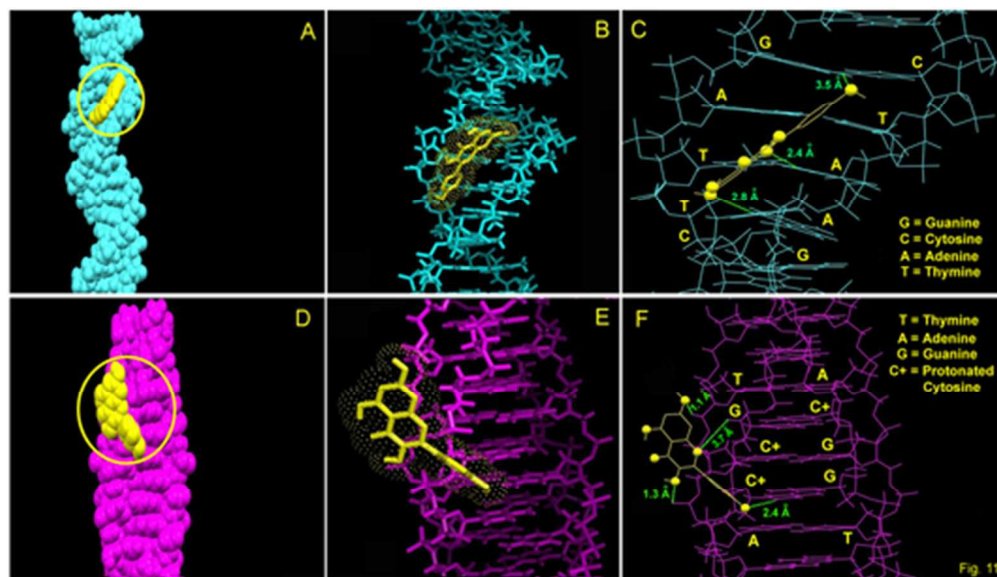


Fig. 10

161x353mm (300 x 300 DPI)



45x25mm (300 x 300 DPI)